the same as the H maser. However, a refrigerated photocell and a He-Ne optical preamplifier should each add about 10 dB. The higher cavity Q will require greater bandwidth in the cavity stabilizing feedback loop, but the signal-to-noise ratio should be ample. With a methane cell of four-times larger aperture, cooled to 76°K, we should closely approximate the H-maser stability.

MANY-BODY THEORY FOR TIME-DEPENDENT PERTURBATIONS IN ATOMIC SYSTEMS*

N. C. Dutta, T. Ishihara, C. Matsubara, and T. P. Das
Department of Physics, University of California, Riverside, California
(Received 5 November 1968)

A many-body approach for the calculation of time-dependent properties of atoms is developed and applied to helium atom. The refractive indices and excitation energies so obtained are in excellent agreement with experiment.

The Brueckner-Goldstone many-body perturbation theory has been used with great success in the past for the calculation of time-independent properties of atoms.[1-3] The purpose of the present Letter is to extend this theory to the calculation of the response of atomic and molecular systems to time-dependent external perturbations. Such a study is of great current interest because of the potential applicability[4] of this response in the calculation of the properties[5-8] of interacting atomic systems. The utilization of diagrammatic techniques in the present method enables us to include and interpret many-electron effects as well as one-electron effects in a systematic way. The procedure is illustrated by the calculation of the frequency dependent polarizability of helium atom. The choice of helium has been dictated by two main reasons. First, helium is the simplest many-body system in which the theory could be tested. Secondly, the results of a number of variational calculations[9-13] and experimental measurements[14-16] are available for both the static and dynamic polarizabilities and optical excitation energies[17] of this atom which can be compared with our theory.

The total Hamiltonian $\mathcal{H}$ for an N-electron atom in the presence of a time-dependent perturbation $\mathcal{H}_2(t)$ is

$$\mathcal{H}=\mathcal{H}_0+\mathcal{H}_1+\mathcal{H}_2(t), \tag{1}$$

where

$$\mathcal{H}_0=\sum_{i=1}^{N}(T_i+V_i),$$

and

$$\mathcal{H}_1=\sum_{i>j}^{N}\frac{1}{r_{ij}}-\sum_{i=1}^{N}V_i. \tag{2}$$

T_i is the sum of the kinetic energy and nuclear Coulomb potential. The single-particle potential V_i, which is in principle arbitrary, is chosen so as to make the perturbation expansion as convergent as possible. To obtain the expectation value of any operator $\mathcal{O}$ for this system, namely,

$$\langle\mathcal{O}\rangle=\langle\Psi(t)|\,\mathcal{O}\,|\Psi(t)\rangle, \tag{3}$$

we need the normalized eigenfunction $\Psi(t)$ of the total Hamiltonian $\mathcal{H}$ in Eq. (1). In obtaining $\Psi(t)$ it is convenient to work in the interaction representation involving the time-development[18] operator $U(t,t_0)$:

$$\Psi(t)=\boldsymbol{U}(t,t_0)\Psi(t_0), \tag{4}$$

where

$$U(t,t_0)=\sum_n U_n(t,t_0),$$

$$U_n(t,t_0)=[(-i)^n/n!]\int_{t_0}^{t}dt_1\cdots\times\int_{t_0}^{t}dt_n\,T\{\mathcal{H}_I(t_1)\cdots\mathcal{H}_I(t_n)\} \tag{5}$$

and $\mathcal{H}_I(t)=e^{i\mathcal{H}_0t}(\mathcal{H}_1+\mathcal{H}_2)e^{-i\mathcal{H}_0t}$, and T is Wick's chronological operator.[18] Using the adiabatic hypothesis,[18] Eq. (3) can be rewritten as

$$\langle\mathcal{O}\rangle=\langle U(t,-\infty)\Phi_0|\,\mathcal{O}_I\,|U(t,-\infty)\Phi_0\rangle=\langle\Phi_0|\,T(\textstyle\sum_n S_n\mathcal{O}_I)\,|\Phi_0\rangle_L, \tag{6}$$

where L indicates that the summation is over linked terms only and $S_n=U_n(\infty,-\infty)$. Φ_0 is the N-particle ground-state eigenfunction of $\mathcal{H}_0$ and is a Slater determinant composed of the lowest N one-electron states in the potential V_i. Using the complete set of eigenstates of $\mathcal{H}_0$, each term in Eq. (6) can be represented by Feynman-like dia-

grams. We shall adopt terminology for diagrams in conformity with earlier applications of Brueckner-Goldstone theory.[1-3]

In the present problem we are interested in the response of an atomic system to a plane-polarized electromagnetic field which has its electric-field component $2E_0\cos\omega t$ in the z direction. In this case $\mathcal{H}_2(t)$ in Eq. (1) has the form

$$\mathcal{H}_2(t)=\sum_{i=1}^{N}(E_0 Z_i e^{i\omega t}+\text{c.c.}), \tag{7}$$

where Z_i is the z coordinate of the ith electron. The frequency-dependent polarizability $\alpha(\omega)$ can be obtained from Eq. (6) by choosing $\mathcal{O}$ to represent the dipole-moment operator $Z=\sum_i Z_i$ in the direction of the field:

$$\langle\Phi_0|T(\textstyle\sum_n S_n Z_I)|\Phi_0\rangle_L = -\alpha(\omega)(E_0 e^{i\omega t}+\text{c.c.}), \tag{8}$$

where $Z_I=e^{i\mathcal{H}_0 t}Ze^{-i\mathcal{H}_0 t}$. For the single-particle potential V_i, we have chosen the V^{N-1}-type Hartree-Fock potential.[1-3] In addition to the occupied bound states, this potential leads to bound and continuum excited states. This choice has proved to be particularly useful from the point of view of convergence of the many-body perturbation expansion in earlier investigations of atomic properties.[1-3]

The diagrammatic expansion of Eq. (8) follows the same lines as for time-independent properties except that the energy denominators associated with the propagators have to be modified[19] because of the time dependence of $\mathcal{H}_2(t)$. Typical diagrams that occur for the polarizability of the ground state of helium are shown in Fig. 1. In these diagrams, the vertices for $\mathcal{H}_2(t)$ and the dipole operator Z_i are represented by "wavy" lines terminating in a dot and a triangle, respectively, while a dotted line is used for the vertex involving $1/r_{ij}$ as in earlier literature.[1-3] The lowest order contribution to $\alpha(\omega)$ arises from the diagram 1(a) which does not involve any correlation or consistence effects. The next higher order diagrams are Figs. 1(b) and 1(c), which represent first-order consistency and correlation effects. Diagrams 1(d) and 1(e) represent second-order correlation effects.

The algebraic expression corresponding to diagram 1(a) is

$$\alpha_0(\omega)=-\sum_{m,k}\left[\frac{\langle m|Z|k\rangle^2}{\epsilon_m-\epsilon_k+\omega}+\frac{\langle m|Z|k\rangle^2}{\epsilon_m-\epsilon_k-\omega}\right] =-2\sum_{m,k}\frac{(\epsilon_m-\epsilon_k)\langle m|Z|k\rangle^2}{(\epsilon_m-\epsilon_k)^2-\omega^2}. \tag{9}$$

The combination of diagrams 1(b) and 1(c) yields

$$\alpha_1(\omega)=-2\sum_{m,m',k,k'}\left[\langle m|Z|k\rangle\langle km'|(1/r_{12})|mk'\rangle\langle k'|Z|m'\rangle\frac{(\epsilon_m-\epsilon_k)(\epsilon_{m'}-\epsilon_{k'})+\omega^2}{\{(\epsilon_m-\epsilon_k)^2-\omega^2\}\{(\epsilon_{m'}-\epsilon_{k'})^2-\omega^2\}}\right.$$
$$\left.+\langle k|Z|m\rangle\langle mm'|(1/r_{12})|kk'\rangle\langle k'|Z|m'\rangle\frac{(\epsilon_m-\epsilon_k)(\epsilon_{m'}-\epsilon_{k'})-\omega^2}{\{(\epsilon_m-\epsilon_k)^2-\omega^2\}\{(\epsilon_{m'}-\epsilon_{k'})^2-\omega^2\}}\right], \tag{10}$$

where m and k denote hole and particle states, respectively. Equations (9) and (10) include the effects of all possible time ordering of the various interaction vertices in each diagram. The expression for $\alpha_2(\omega)$ from diagrams of the type 1(d) and 1(e) are rather cumbersome and will not be presented here.

The evaluation of the diagrams are seen to require matrix elements involving both discrete and continuum excited-state wave functions. These were obtained using techniques described earlier.[2] The summations in Eqs. (9) and (10) involve regular summation for bound excited states and integration over k space for continuum states.[1] At low frequencies, the continuum and bound excited states make comparable contributions, with the $2p$ state providing the major effect. As the frequency increases, the relative contribution from the $2p$ state increases until one reaches the first resonance. Between the first and second resonances, the $3p$ contribution becomes progressively more important, and so on for the higher resonances.

In comparing our results with experiment,[16,17] we shall first consider the refractive index and subsequently the excitation energies. The refractive index $n(\omega)$ for a system of noninteracting at-

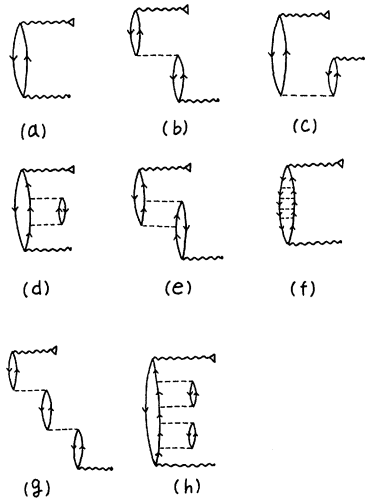

FIG. 1. Diagrams for calculation of frequency-dependent polarizability of helium. For each of the diagrams shown, all possible time orderings of vertices have been included leading to four diagrams of (a), four of (b), four of (c), and 20 of (d) and (e).

oms is related to the atomic polarizability $\alpha(\omega)$ by the relation

$$[n^2(\omega)-1]/[n^2(\omega)+2]=(4\pi/3)N_0\alpha(\omega),$$

where N_0 is the number of atoms per cubic centimeter at standard temperature and pressure. In Fig. 2, we have presented our calculated curve for the refractive index using diagrams 1(a) through 1(e), together with the results of some earlier variational calculations,[5,9-12] and the experimental data of Cuthbertson and Cuthbertson (CC).[16] To enable detailed comparison, the results over the range of frequencies from 0 to 0.2 a.u. are enlarged in the insert in Fig. 2. In comparing theoretical results with experiment, it is important to take account of the pressure variation of the polarizability. The experimental data for $n(\omega)$ shown in Fig. 2 are from the CC measurements at pressures of more than 8 atm. Subsequently, Essen has measured the static polarizability $\alpha(0)$ at 1-atm pressure,[14] and a detailed study of the variation of $\alpha(0)$ with pressure has been carried out by Johnston, Oudemans, and Cole (JOC).[15] The extrapolated value of $\alpha(0)$ for "zero pressure" from the JOC measurements[20] is 1.397, which compares favorably with 1.400 by Essen. On the other hand, by "frequency extrapolation" from the $n(\omega)$ curve of CC, $\alpha(0)$ comes out as 1.384,[21] which is lower than the JOC value. This results is in keeping with the pressure-variation studies of JOC, who found a negative pressure coefficient for $\alpha(0)$ in helium. Since the theoretical calculation refers to the isolated atom, the zero-pressure result of JOC for $\alpha(0)=1.397$ is the appropriate one to compare with theory. Unfortunately no "zero-pressure" data are available for $\alpha(\omega)$, but it is natural to assume that it would also be upgraded from the CC curve by a factor comparable with $\alpha(0)$. Thus, the agreement of our final results including correlation effects is even better than it appears from the in-

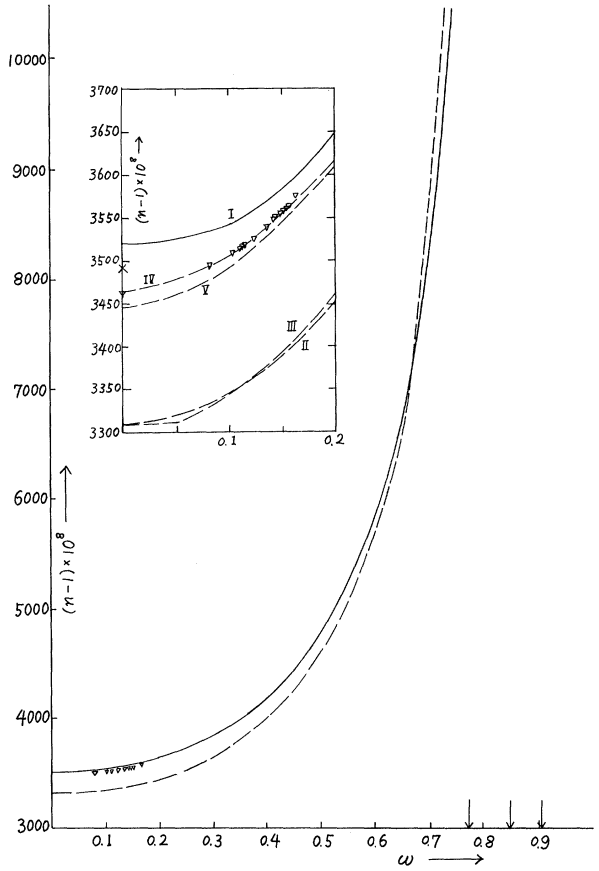

FIG. 2. Variation of $n(\omega)-1$ with angular frequency ω (in atomic units $e^2/a_0\hbar$). In the main plot, the solid curve I represents our final results including correlation effects, the dotted curve II gives the one-electron variational results of Kaveeshwar, Chung, and Hurst (Ref. 11), and the "triangles" represent the experimental results of CC (Ref. 16). The arrows on the ω axis indicate the first two excitation energies and the ionization limit derived from the present calculations. In the enlarged plots in the insert curve III represents the DV one-electron variational results (Ref. 10). Curve IV represents our one-electron results from diagrams 1(a) and 1(b). Curve V represents the CD variational results (Ref. 9) using Hylleraas-type wave functions. The cross and triangles at zero frequency indicate $n(0)-1$ derived from the measurements of JOC (Ref. 15) and CC (Ref. 16), respectively, as explained in the text.

sert in Fig. 2. Among earlier attempts to include correlation in polarizability calculations are those of Chan and Dalgarno (CD)[9] for $\alpha(\omega)$ and Schwartz[13] for $\alpha(0)$. The CD curve for $n(\omega)$, shown in the insert in Fig. 2, is somewhat lower than the CC results. The values of $\alpha(0)$ obtained by CD and Schwartz are 1.383 and 1.377, respectively. Although these values are in close agreement with the "frequency-extrapolated value" of 1.384 from CC data, they are lower than the JOC "zero pressure" value of 1.397. In trying to understand the CD results for $\alpha(\omega)$ with ours including correlation, it should be noted that while they used a correlated Hylleraas-type wave function for the ground state, their perturbed function was, due to practical reasons, limited by the form of the ground-state function, and thus was not flexible enough to include all types of correlation effects. In diagrammatic language, their use of Hylleraas-type ground-state wave function implies that correlation effects of the type in diagram 1(c), associated with the unperturbed state, are included. To include correlation effects associated with the perturbed state as in diagrams 1(d) and 1(e) in a variational procedure would require a trial function which allows the $\vec{r}_{12}$ dependence of the perturbed function to be different from the ground state. Improvements resulting from such a flexible variational function would be interesting for purposes of comparison with our results and experiment. The contribution to $\alpha(\omega)$ from purely one-electron effects can be obtained from our work by combining diagrams 1(a) and 1(b) only. These results are shown in the insert in Fig. 2, and it is interesting that they seem to be in good agreement with the CC data. An alternative procedure for obtaining one-electron contributions to $\alpha(\omega)$ is to solve the fully coupled time-dependent Hartree-Fock perturbation equations derived by Dalgarno and Victor.[10] These equations have, however, been solved so far only approximately by variational procedures,[10-12] in which the results are dependent on the choice of the trial functions. This probably is the reason for the observed difference between our one-electron results and those from the variational calculations.

The singularities in the $\alpha(\omega)$ function are known to yield the excitation energies of the atom, as may also be seen from the energy denominators in Eqs. (9) and (10). To take account of consistency and correlation effects on these energies, we have to include the higher order ladder diagrams of 1(b), 1(d), and 1(e) to infinite order. Examples of such ladders are 1(g) and 1(h). If a V^{N-1} potential had not been used, the ladders in Fig. 1(f) would have had to be included. On including the contributions from ladder diagrams,

Table I. Frequencies of spectral lines of helium.

Transitions $^1S \rightarrow {}^1P$	One-electron theory results[a] (cm^{-1})	Results from diagram (1a) (cm^{-1})	Final Results including consistency & correlation (cm^{-1})	Observed frequency[b] (cm^{-1})	Precentage departure from experiment[c]
$1s^2 \rightarrow 1s2p$	174,811.5	173,455.786	169,831.751	171,129.148	.758%
$1s^2 \rightarrow 1s3p$	189,560.2	189,051.123	185,816.652	186,203.62	.207%
$1s^2 \rightarrow 1s4p$	199,348.8	194,484.650	191,322.003	191,486.95	.086%
$1s^2 \rightarrow 1s5p$		196,990.510	193,869.368	193,936.75	.035%
$1s^2 \rightarrow 1s6p$		198,348.283	195,249.189	195,269.17	.010%
$1s^2 \rightarrow 1s7p$		199,165.488	195,979.521	196,073.41	.048%
$1s^2 \rightarrow 1s8p$		199,695,157	196,539.702	196,595.56	.028%
$1s^2 \rightarrow 1s9p$		200,057.572	196,907.761	196,953.95	.023%
		(An infinite number of other lines obtained in close succession).	(An infinite number of other lines obtained).	(11 other lines have been measured so far).	
Ionization limit	201.466.7	201,419.646	198,247.388	198,305	.029%

[a]See Ref. 12.
[b]See Ref. 17.
[c]Departure from experiment = [(column 5−column 4)/column 5]×100.

the energy denominators of Eq. (9) are modified to the forms $(\epsilon_{1s}-\epsilon_k)^2+\sum_i\Delta_i-\omega_k^2$ which lead to the singularities

$$\omega_k=\{(\epsilon_{1s}-\epsilon_k)^2+\textstyle\sum_i\Delta_i\}^{1/2}, \tag{11}$$

where Δ_i is the ratio of the contribution to $\alpha(\omega)$ from the first member of the ith family to the parent diagram 1(a). These singularities are infinite in number corresponding to the infinite number of bound excited states of the atom. Nine of these energies predicted by Eq. (11) are compared in column IV of Table I with experimentally observed excitation energies[17] in column V and the agreement is seen to be very good. Actually, 19 excitation energies and the ionization potential have been measured so far and they are all in excellent agreement with our results. Again, if one wanted to analyze the role of one-electron effects only, one would have to combine the diagrams 1(a), 1(b), and the ladder 1(g) associated with the latter. The singularities from diagram 1(a) are equal to the infinite number of excited p-state energies in the V^{N-1} potential and as seen from Table I, they are already in quite good agreement with experiment. Inclusion of the effects of the diagrams 1(b) and 1(g) would push the singularities closer to column IV and experiment. Again, the excitation energies associated with one-electron effects can be obtained by solving the Dalgarno-Victor equations exactly. However, they have only been solved variationally for this purpose by Sengupta and Mukherji.[12] These authors obtained only three of the expected infinite excitation energies as indicated in column II of Table I. This result is a stronger manifestation of the sensitiveness of variational calculations to the choice of trial functions than was the case for the $\alpha(\omega)$ function.

In summary, the Breuckner-Goldstone method, as adapted here for time-dependent problems, appears to be particularly convenient for the evaluation of atomic properties including many-body effects. We have applied it here successfully to calculate the frequency-dependent polarizability and excitation energies of helium. The real power of this technique will be manifested in applications to heavier atoms where many-body effects are expected to be more important.

*Work supported by the National Science Foundation.

[1]H. P. Kelly, in Perturbation Theory and its Applications in Quantum Mechanics, edited by C. H. Wilcox (John Wiley & Sons, Inc., New York, 1966), p. 215, and Phys. Rev. 131, 684 (1963), and 136, B896 (1964), and 173, 142 (1968), and references therein.

[2]N. C. Dutta, C. Matsubara, R. T. Pu, and T. P. Das, Phys. Rev. Letters 21, 1139 (1968), and Phys. Rev. (to be published).

[3]E. S. Chang, Robert T. Pu, and T. P. Das, Phys. Rev. 174, 1, 16 (1968).

[4]C. Mavroyannis and M. J. Stephen, Mol. Phys. 5, 629 (1962).

[5]M. Karplus and H. J. Kolker, J. Chem. Phys. 39, 1493, 2997 (1963).

[6]Michael O'Carroll and Joseph Sucher, Phys. Rev. Letters 21, 1143 (1968).

[7]Robert O. Garrett, Shang Yi Ch'en, and Eng Choon Looi, Phys. Rev. 156, 48 (1967), and references therein.

[8]R. A. Brown and F. M. Pipkin, Phys. Rev. 174, 48 (1968); J. D. Lyons, Supriya Ray, and T. P. Das, ibid. 174, 104 (1968), and references therein.

[9]Y. M. Chan and A. Dalgarno, Proc. Phys. Soc. (London) 85, 227 (1965).

[10]A. Dalgarno and G. A. Victor, Proc. Roy. Soc. (London), Ser. A 291, 291 (1966).

[11]V. G. Kaveeshwar, Kwong T. Chung, and R. P. Hurst, Phys. Rev. 172, 35 (1968).

[12]S. Sengupta and A. Muhkerji, J. Chem. Phys. 47, 260 (1967).

[13]C. Schwartz, Phys. Rev. 123, 1700 (1961).

[14]L. Essen, Proc. Phys. Soc. (London), Ser. B 66, 189 (1953).

[15]D. A. Johnston, C. J. Oudemans, and R. H. Cole, J. Chem. Phys. 33, 1310 (1960).

[16]C. Cuthbertson and M. Cuthbertson, Proc. Roy. Soc. (London), Ser. A 135, 40 (1932).

[17]The experimental values of the transition frequencies are tabulated by Charlotte E. Moore, National Bureau of Standards Circular No. 467 (U.S. Government Printing Office, Washington, D.C., 1949), Vol. 1.

[18]See Silvan S. Schweber, An Introduction to Quantum Field Theory (Harper and Row Publishers, Inc., New York, 1962), Chaps. 6 and 11.

[19]A more detailed discussion of the procedure will appear in a subsequent publication dealing with the properties of interacting atoms.

[20]All values for polarizabilities are quoted in atomic units. In obtaining them from measured refractive indices we have used $N_0=0.268\,70\times10^{20}$ and the Bohr radius $a_0=5.291\,67\times10^{-9}$ cm from Phys. Today 71, No. 2, p. 48 (1964).

[21]A. Dalgarno and A. E. Kingston, Proc. Roy. Soc. (London), Ser. A 259, 424 (1960).